Droplet ejection in laser-induced forward transfer: mechanism for droplet fragmentation

***R. Pohl*[1], *C.W. Visser*[2], *G.R.B.E. Römer*[1], *C. Sun*[2], *A.J. Huis in't Veld*[1,3], *D. Lohse*[2]**

[*1] *Chair of Applied Laser Technology, Faculty of Engineering Technology, University of Twente, The Netherlands*
[*2] *Physics of Fluids, Faculty of Science and Technology, Mesa+ Institute, University of Twente, The Netherlands*
[*3] *TNO Technical Sciences, Mechatronics, Mechanics and Materials, The Netherlands*

Laser-induced forward transfer is a direct-write method suitable for precision printing of various materials. However, occasional defects (i.e. contamination of the receiver due to the impact of multiple small droplets instead of a single droplet) hamper a widespread application of this method. As the ejection mechanism has not been visualized in detail, the cause of these defects is not understood as yet. Therefore, this article presents an experimental study on the ejection process mechanisms of copper-based picosecond laser-induced forward transfer. Images were obtained using bright field illumination by a 6 ns pulsed laser and a 50× long-distance microscope objective. For laser fluences just above the transfer-threshold, the release of a single droplet is frequently (97%) observed. The typical droplet radius in these cases is estimated to be 3 µm. However, images acquired at a later time in time show multiple droplets in the majority (86%) of the observations. The droplet fragments usually follow the main droplet. Two mechanisms to explain these fragments are proposed: i) break-up of "threads" between the donor layer and the ejected droplet; ii) contraction of the ejected droplet. As the phase of the ejected copper is not identified completely, the exact mechanism is not yet known and will be subject of further research.

Keywords: LIFT, metal printing, droplet ejection, time-resolved imaging

1. Introduction

Laser-induced forward transfer (LIFT) is a high resolution 3D direct write printing method that was demonstrated first in 1986[1]. LIFT involves a transparent substrate (carrier) which is coated with a thin film (donor). The carrier is placed close to a second substrate (receiver). A pulsed laser beam is focused through the transparent carrier onto the carrier-donor-interface. Laser energy is absorbed within a thin layer of the donor material. If the laser fluence is sufficiently high, the donor material is ejected and propelled towards the receiving substrate.

This technique allows transfer of a range of various materials by the deposition and subsequent solidification of molten droplets. However, despite decades of research, the ejection during the LIFT process is not fully controlled and therefore hardly implemented. Persistent defects, i.e. contamination on the receiving substrate, hamper a wide spread use of this technique. So far, the majority of experiments are based on post process analysis, i.e. the inspection of the deposited droplets on the receiving substrate or the donor layer. In literature, two main theories[2,3] try to explain the release process: (*i*) creation of vapor/plasma at the carrier donor interface; (*ii*) and the relaxation of thermally induced stresses. It is unknown under which conditions these phenomena occur. Time-resolved observations of LIFT processes of Au[4], Ni[5] and Cr[6] do not achieve sufficient spatial resolution to follow the process in detail. In this article we present time-resolved images showing the ejection process at fluences just above the transfer threshold.

2. Experimental Setup

Experiments were performed using an Yb:YAG laser source with a fixed pulse duration of 6.7 ps, a central wavelength of 515 nm (SHG) and a Gaussian beam profile with a beam quality measured to be M^2<1.3. The pulsed laser beam was focused onto the carrier-donor interface using a 100 mm f-theta scan-lens that was attached to a 2D galvo-scanner. The focused beam waist ($1/e^2$) was measured to be 8.3±0.6 µm. A 1 mm thick soda-lime glass substrate, sputtered with a 200 nm thick copper film, was used as the donor-layer, see figure 1. For the benefit of image quality, no receiving substrate was used. Images were recorded using a dual-shot CCD camera, mounted to a standard 200 mm tube lens and a 50× long-distance objective. As an illumination source, an incoherent strobe pulse was generated by a dual-cavity Nd:YAG laser that was combined with a high efficiency diffuser.[7] This results in a diffuse bright-field illumination with an exposure time of 6 ns per frame. A pulse/delay generator was used to ensure a proper timing of the strobe pulse and the shutter of the camera with respect to the incident 515nm LIFT laser pulse, see figure 1. Trigger sequences were started by the output of a photodiode connected to the LIFT laser beam path. Although the triggering sequence was optimized, a temporal jitter between separate ejection events was estimated to be 50 ns. However, due to the combination of a dual-shot

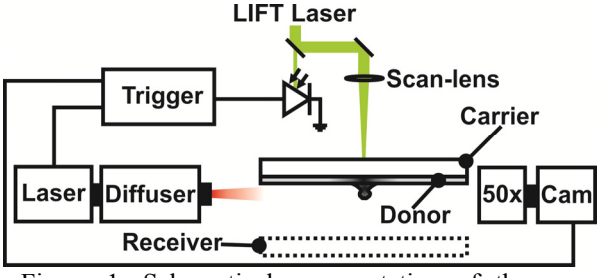

Figure 1: Schematical representation of the exeprimental setup

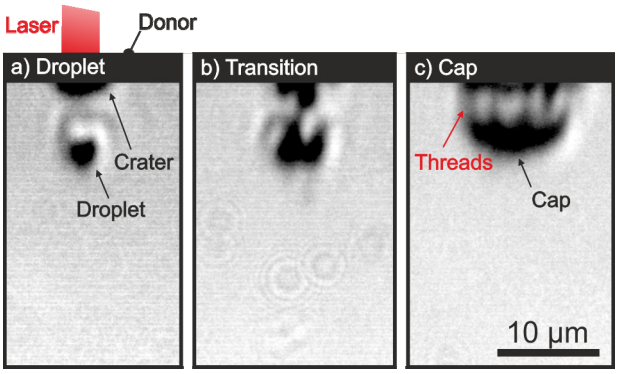

Figure 2: Ejection phenomena at laser fluences of (a) 188 mJ/cm^2, (b) 207 mJ/cm^2 and (c) 222 mJ/cm^2.

camera with a dual-cavity strobe illumination source, each ejection event has been imaged twice (referred to in the following as image A and B). The temporal delay between these A- and B-images was set to 350 ns.

3. Results and Discussion

This section presents images that were obtained at fluences varying from the ejection-threshold fluence up to 2.5 times this threshold. First, typical ejection phenomena which were observed within this fluence range will be shown. Next, time-resolved A- and B-image sequences, that indicate the ejection and fragmentation of the ejected droplets or caps, will be shown. This fragmentation, i.e. the creation of multiple droplets is further analyzed and discussed afterwards. Finally, measurements of the droplet velocities are presented and interpreted using a simple fit.

3.1 Droplet and Cap-like ejection

Figure 2 shows three ejection phenomena obtained at fluences of 188 mJ/cm^2, 207 mJ/cm^2 and 222 mJ/cm^2, respectively. The timing was set to 50 ns with respect to the first visible deformation of the donor layer. In this figure, the 200 nm thick donor layer is indicated by the black horizontal bar (top). Note that its thickness is not drawn in scale. Figure 2(a) shows an almost spherical droplet that is fully detached form the donor layer. The diameter of the droplet is estimated to be 3 µm. With increasing fluence a variation in the size and the shape of the ejected material can be observed. Figure 2(c) indicates a half-spherical shaped ejection, which is referred to as "cap ejection" in the following. The cap seems to be still partly attached to the donor layer, as thin "threads" between the cap and the donor layer are visible. These threads are frequently observed in liquid sheet experiments, indicating that the copper is liquid at this instance. The width of the observed cap is estimated to be 10 µm.

In both cases, the width of the ejected droplet/cap matches the observed crater formation at the interface of the donor-layer. The ejected volume is estimated by the donor layer thickness and the observed crater size. The volume of the observed ejections can be estimated by assuming a spherical and half-spherical shape of the droplet and cap, respectively. A volume comparison reveals a significant mismatch in volume. Hence, it is likely to assume

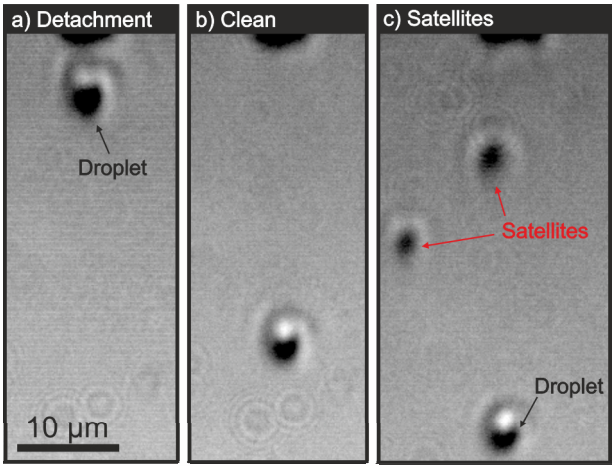

Figure 3: Droplet fragmentation

that the ejections are hollow at this instance. In literature the ejection of liquid metals using the femtosecond LIFT process at the threshold fluence has been visualized for relatively thin layers. The dominant physics was found to be the relaxation of laser-induced stresses[8]. The ejection by a picosecond laser pulse presented in figure 2(a) does not indicate a jet forming as it was reported elsewhere for low fluence femtosecond LIFT ejections. It should be noted that the current results were obtained using a relatively thick donor layer (200 nm) when compared to the heat affected zone. In contrast to relatively thin layers (e.g. 50 nm) such a thick layer exhibits a significant temperature gradient along the penetration axis when heated by picosecond laser pulse. Hence, it is proposed that the observed ejection process is dominated by the formation of a vapor bubble instead of stress relaxation.

3.2 Fragmentation

Figure 3 shows images that were acquired at a fixed laser fluence of 188 mJ/cm^2. Figure 3(a) shows the A-image of an ejected droplet using similar settings as in figure 2(a). The droplet is observed in close proximity to the donor layer. Except for threads, no additional droplets or fragments are visible. Figure 3(b) and 3(c) are the B-image of the dual-shot camera and were recorded with a time delay of 350 ns with respect to the image shown in figure 3(a). The B-images were chosen to indicate two typical observations that have been made during the experiments. Namely:

i) Clean ejection: Figure 3(b) shows a single droplet slightly shifted with respect to the droplet in figure 3(a). No, additional droplets visible.

ii) Satellites: Figure 3(c) indicates a main droplet that is followed by two additional, relatively smaller droplets. These additional droplets are referred as satellites.

Figure 4 (a) shows the ejection of a cap, as already shown in figure 2(c). Besides the threads at the rupture of the cap and the donor layer, no additional droplets or fragments are visible. Figures 4(b) and 4(c) are again the B-image of the dual-shot imaging setup. The time delay was fixed at

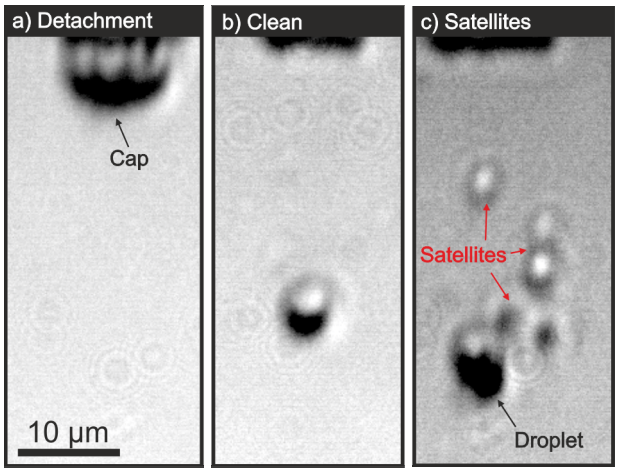

Figure 4: Cap fragmentation

350 ns to the A-image. Again, these images were chosen to demonstrate two typical ejection events that have been observed.

i) Clean: Figure 4(b) shows a droplet slightly dislocated with respect to the cap in figure 4(a). The diameter of the droplet decreased significantly and the cap contracted to a droplet like shape.

ii) Satellites: Figure 4(c) shows a deformed major droplet near the bottom of the image. This droplet is followed by additional "blurry events", which are interpreted here as small droplets, i.e. satellites.

The observed satellites in the B-images of figures 3 and 4 are likely to cause contaminations, i.e. undesired depositions on a receiving substrate. For further statistical investigations, 220 image pairs (A- and B-images) have carefully been analyzed. That is, from each image the following data was extracted: Ejection type (droplet or cap), crater location/size, droplet/cap location and the number and location of additional droplets (i.e. satellites).

Figure 5(a) shows the observed number of droplets in each A image, i.e. at the detachment or shortly after, as a function of the laser fluence. The timing was kept at a fixed value of 50 ns. The plot shows no dependency of the laser fluence on the number of observed droplets/caps.

Figure 5 (c) shows a histogram of the data in figure 5(a) – indicating the frequencies of observed single and multi-droplet ejections. As already indicated in figure 5 (a), ejections with more than one droplet/cap occasionally occur, but are rarely observed (3%). The majority (97%) of the images have been identified as being single droplet/cap ejection events. However, figure 5(b) presents the number of droplets in each B image, i.e. the ejection stage at 350 ns after image A. Despite the strong variation of the data, a trend of an increased number of droplets towards higher

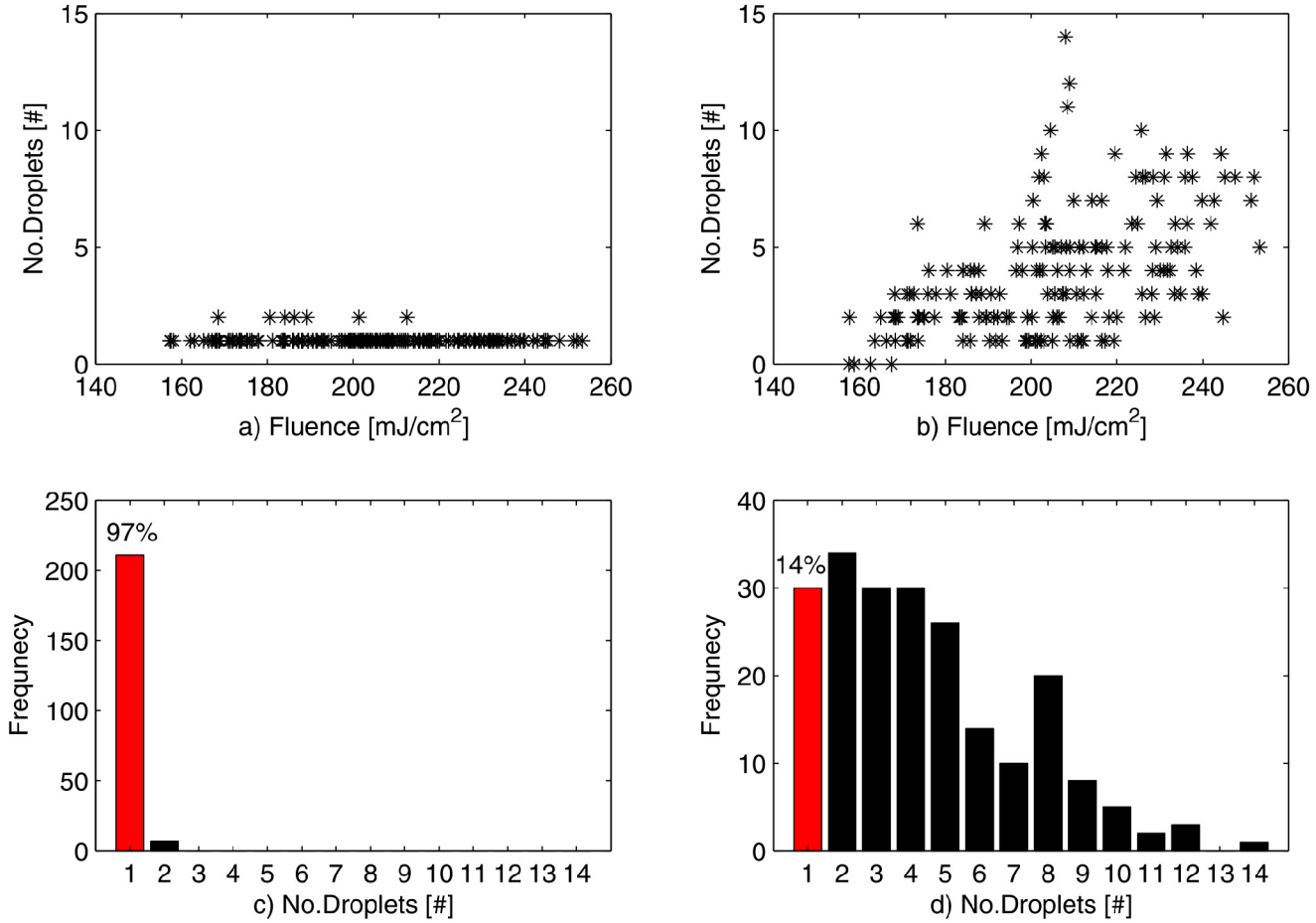

Figure 5: (a) Image-A and (b) Image-B: Number of ejection events as a function of laser fluence; (c) and (d) histograms of the data in (a) and (d), respectively;

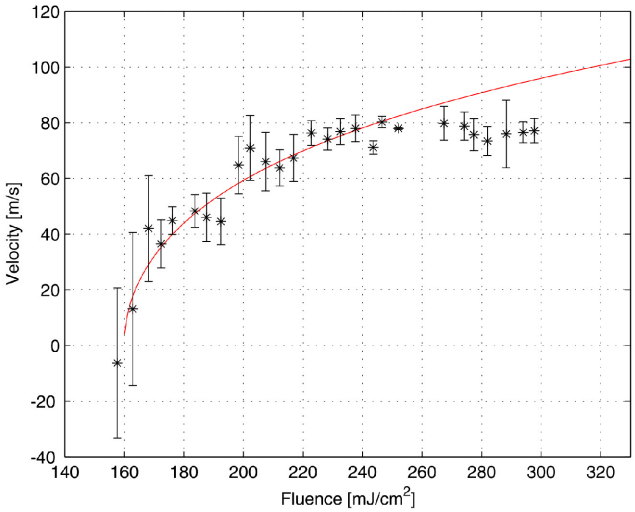

Figure 6: Droplet and cap velocity

fluences can be identified. Moreover, the corresponding histogram in Figure 5(d) indicates a significant decrease (14%) of single droplet/cap observations. Whereat, the majority (86%) of the images show multiple droplets. This suggests that the single droplet is breaking up within a time scale of 350ns. Based on two different observations, we propose two possible mechanisms for this break-up:

i) Breakup of threads during the detachment: As shown in figure 2 (c) threads are visible along the rupture between the cap and the crater. If liquid, these threads are unstable and will break up into droplets. This is called the Rayleigh-Plateau instability. A typical time scale was estimated to be 100 ns[i], i.e. matching our observations.

ii) Break-up of the droplet. As discussed, the droplets ejected are hollow. This implies that the droplets consist of a liquid sheet. Any liquid sheet is instable, as deviations from its initial (homogenous) thickness are amplified similar to Rayleigh-Plateau break-up of a liquid thread. A time scale for this break-up was included in Keller et al. [10], and for our case estimated as 200 ns[ii]. This also matches our observations.

From our measurements, we observed that the satellites reported here and earlier are an in-flight phenomenon. This strongly suggests break-up of threads or the metal sheet is the governing mechanism. However, as yet, we cannot distinguish between these mechanisms. To obtain more accurate time- and length scales, we are currently numerically modeling the sheet behavior.

3.3 Velocity measurements

Based on the droplet and cap locations in the A- and B-images of each ejection event, the velocity was determined. Figure 6 shows the velocity of the ejected droplets/caps as a function of the laser fluence applied. Each data point corresponds to the median fluence value of a set of data points contained in an interval of 5 mJ/cm^2. The velocity is calculated as the median velocity of the corresponding fluence interval. The error-bars indicate the standard deviation of the velocity for a given interval. To a first approach, the observed square-root like trend was fitted with a simple model. Therefore, the velocity v is expressed by the law of kinetic energy of the droplet(s):

$$v = \sqrt{\frac{2 \times A \times (F_{laser} - F_{th})}{m \times \ln(F_{laser} / F_{th} \times \exp(1))}}\ , \qquad (1)$$

where A is the irradiated area given by the spot size (1/e^2) of the laser, m represents the ejected mass and F_{laser} and F_{th} correspond to the averaged incident laser and threshold fluences, respectively. The natural logarithm is used to represent the variation of the ejected mass, given by the Gaussian beam distribution of the focused laser. Based on this fit the transfer fluence threshold is determined to be 159 mJ/cm^2. The maximum velocity is found to be about 80 m/s for a given laser fluence of about two times the F_{th}. Besides the threshold fluence, also the ejected mass was used as a fitting parameter. A comparison of the ejected mass with respect to the mass given by the spot size of the focused laser and the donor layer thickness reveals a value of 0.42. The value seems to be in the right order of magnitude to support the proposed fit. Future investigations will contain the deviations of the data from the fit starting at fluences above 250 mJ/cm^2 – indicating additional physics to become relevant for the ejection process. Further discussions on this topic are out of the scope of this paper.

4. Conclusions

An experimental study on the low fluence ejection mechanism of LIFT was presented. Two different ejection phenomena (droplets and caps) have been observed. Time-resolved images indicate a mechanism, causing the ejected droplets/caps to fragmentize. The breakup of "threads" and the contraction of the ejected droplets/caps are proposed to explain the observed fragmentation. A maximum droplet velocity was found to be about 80 m/s at a laser fluence of about two times F_{th}. Based on a physical simple fit the transfer threshold was estimated to be 159 mJ/cm^2.

Acknowledgments and Appendixes

R. Pohl, G.R.B.E. Römer, and A.J. Huis in't Veld are grateful to the European Union Seventh Framework Programme for the funding under Grant Agreement No. 260079. (www.fab2asm.eu) C.W. Visser, Chao Sun and Detlef Lohse acknowledge Fundamenteel Onderzoek der Materie (FOM) for funding.

References

[1] J. Bohandy, B. F. Kim, and F. J. Adrian, J. Appl. Phys. 60 (1986) 1538.

[2] V.P. Veiko, E.A. Shakhno, V.N. Smirnov, A.M. Miaskovski, and G.D. Nikishin, Laser and Particle Beams 24 (2006) 203-209.

[3] Tobias C. Röder, and Jürgen R. Köhler, Appl. Phys. Lett. 100 (2012) 071603.

[4] Y. Nakata, T. Okada, Appl. Phys. A 69 (1999) 275-278.

[5] T. Sano, H. Yamada, T. Nakayama, I. Miyamoto, Appl. Surf. Sci. 186 (2002) 221-226.

[6] I. Zergioti, D.G. Papazoglou, A. Karaiskou, C. Fotakis, E. Gamaly, A. Rode, Appl. Surf. Sci. 208-209 (2003) 177-180.

[7] Arjan van der Bos, Aaldert Zijlstra, Erik Gelderblom, Michel Versluis, Exp Fluids 51 (2011) 1283-1289.

[8] Arseniy I. Kuznetsov, Claudia Unger, J. K. & Chichkov, B. N., Appl Phys. A 106 (2012) 479-487.

[9] Formula used from Eggers, Jens. "Nonlinear dynamics and breakup of free-surface flows." *Reviews of modern physics* 69.3 (1997): 865.

[10] Keller, Joseph B., and Ignace Kolodner. "Instability of liquid surfaces and the formation of drops." *Journal of Applied Physics* 25.7 (1954): 918-921.

---

[i] *sigma = 0.7;* %surface tension
rho = 8e3; %density
g = 10; %Gravitational acceleration
dt = 100e-9; %typical time scale
dx = 10e-6; %typical length scale
a = dx/dt^2; %resulting typical acceleration
h = 200e-9; %Sheet thickness 200nm
A = 1e-10; %initial perturbation (0.1nm - one atomic length)
r0 = 1e-6; %Initial thread radius

%Rayleigh 1879 a and b (by Eggers), for threads
*tau_RP = sqrt(r0^3*rho/sigma)*

%Keller 1954, for sheets
[ii] *tau_Keller =*
*(27*sigma/(4*rho*(abs(a+g)^3)))^(1/4)*log(h/A)*